

SWIFTDIFFUSION: Efficient Diffusion Model Serving with Add-on Modules

Suyi Li*, Lingyun Yang*, Xiaoxiao Jiang, Hanfeng Lu, Dakai An, Zhipeng Di[◇], Weiyi Lu[◇], Jiawei Chen[◇]
 Kan Liu[◇], Yinghao Yu[◇], Tao Lan[◇], Guodong Yang[◇], Lin Qu[◇], Liping Zhang[◇], Wei Wang[◇]
 HKUST, [◇]Alibaba Group

Abstract

Text-to-image (T2I) generation using diffusion models has become a blockbuster service in today’s AI cloud. A production T2I service typically involves a serving workflow where a base diffusion model is augmented with various “add-on” modules, notably ControlNet and LoRA, to enhance image generation control. Compared to serving the base model alone, these add-on modules introduce significant loading and computational overhead, resulting in increased latency. In this paper, we present SWIFTDIFFUSION, a system that efficiently serves a T2I workflow through a holistic approach. SWIFTDIFFUSION decouples ControlNet from the base model and deploys it as a *separate, independently scaled service on dedicated GPUs*, enabling ControlNet caching, parallelization, and sharing. To mitigate the high loading overhead of LoRA serving, SWIFTDIFFUSION employs a *bounded asynchronous LoRA loading (BAL)* technique, allowing LoRA loading to overlap with the initial base model execution by *up to k steps* without compromising image quality. Furthermore, SWIFTDIFFUSION optimizes base model execution with a novel *latent parallelism* technique. Collectively, these designs enable SWIFTDIFFUSION to outperform the state-of-the-art T2I serving systems, achieving up to $7.8\times$ latency reduction and $1.6\times$ throughput improvement in serving SDXL models on H800 GPUs, without sacrificing image quality.

1 Introduction

Text-to-image (T2I) generation using diffusion models is a transformative AI technology that enables the creation of high-quality, contextually accurate images from textual descriptions. This technology has gained immense popularity, with a variety of prominent T2I services available in the cloud, such as DALL·E [30], Midjourney [29], and Firefly [6]. Notably, Firefly has reportedly generated over 2 billion images [5], highlighting the significant demand for T2I services.

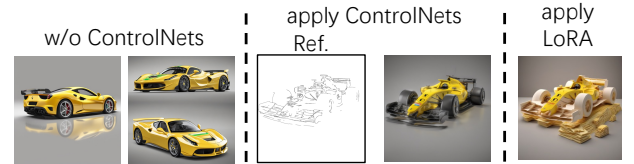


Figure 1: Effects of ControlNet and LoRA in image generation with SDXL under the same prompt: racing game car, yellow Ferrari. **Left:** without ControlNet, the generated images can have different compositions. **Center:** ControlNet uses a reference image to control the composition. **Right:** using LoRA to generate image in a papercut style.

A production T2I service typically consists of multiple components. At its core is a base stable diffusion model [12, 24, 32]. This model is trained to produce a coherent image through a *reverse diffusion process* [33]: it starts with an image composed of random noises and progressively denoises this random input in iterations, until the output image aligns with the provided text description. In addition to the base diffusion model, production T2I services provide various “add-on” modules, including ControlNet [57] and LoRA (Low-Rank Adaptation [19]), that allow users to control the details of the output images, such as shapes, outlines, poses, and styles. Fig. 1 illustrates the effects of using these two modules. ControlNet allows users to input a reference image to guide the spatial composition of the generated image, while LoRA produces an image with customized stylistic effects. In our production platform, over 98% of requests demand at least one ControlNet, and over 95% utilize at least one LoRA (§3).

The base diffusion model, together with the requested add-on modules, compose a *T2I serving workflow*. However, the use of these add-on modules poses new challenges. To illustrate this, we configure a T2I workflow where a base SDXL model [32] is augmented with a varying number of ControlNets and LoRAs. Fig. 2 depicts the serving latency of these workflows (blue bar). Compared with serving the base model alone (0C/0L), serving it together with add-on modules results in a significant delay, which is increasing as more ControlNets

*Equal contribution

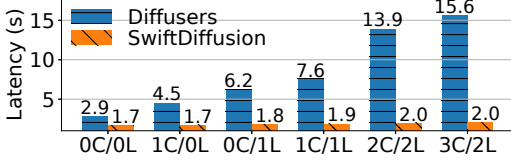


Figure 2: **ControlNets and LoRAs introduce additional latency overhead.** In each workflow, a common base SDXL [32] model is augmented with m ControlNets and n LoRAs (mC/nL), served by Diffusers [42] on an H800 GPU.

and LoRAs are in use. This delay mainly comes from two sources. **First**, as the desired ControlNets and LoRAs vary across requests, they must be fetched from storage and loaded into GPU memory before serving, introducing significant loading overhead. In our production platform, each request undergoes one ControlNet loading and one LoRA loading on average, which account for 37% of the end-to-end serving latency (§3). Note that pre-caching all add-on modules in GPU memory is *infeasible*: our production trace reports nearly 150 distinct ControlNets and 14,500 LoRAs requested by users; each ControlNet is around 3 GiB and each LoRA is hundreds of MiB¹. **Second**, while LoRA is lightweight, ControlNet is compute-intensive. Fig. 2 shows that using one ControlNet in T2I generation adds 1.6 seconds to the serving latency, which is $1.5\times$ longer than serving the base model alone (2.9 seconds). As more ControlNets are utilized, their computational overhead accumulates, leading to a significant latency increase (Fig. 2).

Despite these challenges, efficiently serving a T2I workflow with add-on modules has been largely unexplored; prior work primarily focuses on improving the serving latency and image quality of a single base diffusion model [7, 22, 42, 48]. In this paper, we propose SWIFTDIFFUSION, a system that efficiently serves a base diffusion model and the associated ControlNets and LoRAs for enhanced image generation control. SWIFTDIFFUSION employs a holistic approach with three novel designs driven by a characterization study in a production platform (§3):

ControlNet-as-a-Service. Efficient ControlNet serving requires addressing the GPU loading and computational overhead. Our characterization study reveals that ControlNets exhibit the *skewed popularity*; that is, a small number of ControlNets (9–11%) are invoked frequently by a large number of user requests (95–98%). Caching these popular ControlNets in GPU memory effectively reduces the loading tax, with only modest memory footprint. To accelerate computation, SWIFTDIFFUSION *concurrently executes* ControlNet(s) with the base diffusion model on *multiple GPUs*, achieving *close-to-ideal speedup* compared to the current sequential execution schemes [42].

SWIFTDIFFUSION implements ControlNet caching and parallelization with a new design called *ControlNet-as-a-Service*.

¹The ControlNets and LoRAs are for the SDXL model.

It decouples ControlNets from the base model and deploys them as a *separate, independently scaled service on dedicated GPUs*, where popular ControlNets are cached in GPU memory to eliminate the loading overhead. This service can be dynamically invoked to execute desired ControlNets in parallel with the base model. This design additionally enables *ControlNet sharing*, in that a single ControlNet can be multiplexed by multiple base models.

Bounded asynchronous LoRA loading. Unlike ControlNet, LoRA is compute-light and LoRA serving is mainly bottlenecked by the loading overhead. Given their large populations, LoRA adapters are usually maintained in disk or remote memory storage and must be brought into GPU memory on-demand. We notice that LoRA caching offers limited benefits in this scenario as LoRA adapters exhibit a *heavy-tailed distribution in popularity* (§3.2).

To address this challenge, we analyze the T2I generation process with and without LoRAs and find that the two computations diverge largely in the *later stage* of the denoising process. This suggests that one can exclude LoRA computation in initial steps and include them only in latter iterations, while still producing images of the same quality. Based on this insight, we propose *bounded asynchronous LoRA loading* (BAL). That is, while the requested LoRAs are being loaded into GPUs, SWIFTDIFFUSION asynchronously executes the base model (and the desired ControlNets, if any) to early start the image generation process without LoRA by *up to k steps*, beyond which LoRA computation must be included to continue the remaining generation steps. By tuning the asynchronous bound k , SWIFTDIFFUSION effectively overlaps LoRA loading with base model execution, without compromising image quality (§6.2).

Latent parallelism for CFG computation. In addition to add-on modules, SWIFTDIFFUSION optimizes base model execution with a new parallelism technique. As mentioned earlier, T2I generation is essentially a denoising process, where the diffusion model progressively refines a *latent tensor*, initially filled with random noise, through multiple denoising steps [12, 24, 32]. Each denoising step employs the classifier-free guidance (CFG) to effectively improve image quality and alignment [18]. In CFG, the input latent tensor is duplicated and the two replicas undergo two different denoising processes, one guided by the text prompt (conditioned denoising) and the other not (unconditioned denoising). The two denoised tensors are then aggregated by computing a weighted sum. Since conditioned and unconditioned denoising have no dependency, SWIFTDIFFUSION parallelizes the two computations on two GPUs. This *latent parallelism* technique can also be applied to accelerate the CFG computation in ControlNet serving. This technique, together with other engineering optimizations, collectively accelerate base model execution by $1.7\times$ (§6.5).

We have implemented SWIFTDIFFUSION on top of Hug-

Add-on Module	Number	Service A	Service B
ControlNet	0	0	1.9%
	1	30.5%	25.1%
	2	69.5%	69.9%
	3	0	3.1%
LoRA	0	0.2%	7.2%
	1	8.8%	73.6%
	2	91%	19.2%

Table 1: The distribution of the number of ControlNets and LoRAs used by each request in two production services.

cally, given a pre-trained weight matrix $\mathbf{W} \in \mathbb{R}^{H_1 \times H_2}$ in a base model, LoRA introduces two low-rank matrices $\mathbf{A} \in \mathbb{R}^{H_1 \times r}$ and $\mathbf{B} \in \mathbb{R}^{r \times H_2}$, where r is the LoRA rank. By modifying the weight matrix to $\mathbf{W}' = \mathbf{W} + \mathbf{AB}$, LoRA effectively stylizes the final generated image, infusing it with the desired visual characteristics.

Other add-on modules. Our work primarily focuses on ControlNet [57] and LoRA [19], two widely adopted add-on modules in our production platform (§3). Meanwhile, there are emerging add-on modules [2, 21, 44, 52, 58] introduced by the research community to control image generation, most of which are developed based on UNet architectures [12, 32, 34]. These modules can be broadly categorized into two groups. The first group comprises models that operate in tandem with the base model during inference, akin to ControlNet. Representative examples include IP-Adapter [52], InstantID [44], and BrushNet [21]. The second group consists of models that augment the base model by incorporating parameter-efficient patches, similar to LoRA. Examples include Fooocus Inpaint [2] and IC-Light [58]. Notably, the techniques proposed in SWIFTDIFFUSION are generalizable and can be adapted to support these alternative add-on modules.

3 Characterization Study

In this section, we present a characterization study on a 20-day workload trace collected in May and June 2024 on a production platform. The trace contains more than 500k inference requests to two core T2I services for online retailing applications.² Our characterization not only reflects the deployment scenarios of diffusion models in production, but also reveals the inefficiency of current T2I serving systems.

3.1 ControlNet Characterization

Prevalence. Table 1 shows the distribution of the number of ControlNets utilized by each request in two services. ControlNet is used by almost all requests for image generation control; approximately 70% of these requests utilize two or more ControlNets simultaneously.

Skewed popularity. Compared to a large quantity of requests, only 141 ControlNets are used in two services, where

²We are working on releasing the trace for public access.

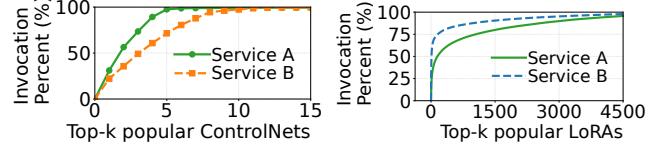


Figure 4: **Left:** ControlNet has a small population and exhibits a skewed popularity; the long tail of the graph is truncated for a better presentation. **Right:** LoRA has a large quantity and exhibits a long-tailed distribution in popularity.

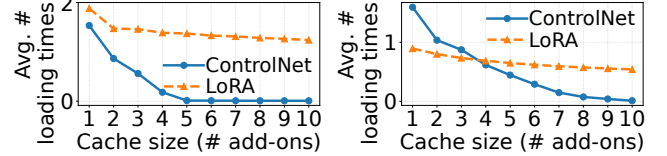


Figure 5: ControlNet loading overhead can be alleviated using a larger LRU cache, while LoRA performance gains are less pronounced. **Left:** Service A; **Right:** Service B.

Service A offers 47 distinct ControlNets and Service B provides 94. These ControlNets exhibit a severe imbalance in access frequency, with a handful of ControlNets being extremely popular (Fig. 4-Left). In Service A, the top-5 popular ControlNets (11% in population) account for 98% of total invocations; in Service B, the top-8 popular ControlNets (9% in population) contribute to 95% of total invocations.

The need for ControlNet caching. ControlNets are large in size (3 GiB each) and usually maintained in remote storage, introducing significant loading overhead. Given that ControlNets have a limited quantity and skewed popularity, caching top popular ControlNets in GPU memory can effectively reduce the loading overhead. To illustrate this, we configure an LRU cache of varying size for ControlNet caching. We replay the trace and measure the average number of times that the desired ControlNets are not resident on GPU and must be fetched from storage (i.e., cache miss) when serving two consecutive requests that desire different ControlNets. As illustrated in Fig. 5 (blue curves), caching only a handful of top popular ControlNets is sufficient to eliminate the loading overhead (top-5 for Service A and top-8 for Service B).

Computational overhead. ControlNet is compute-intensive as it shares a similar architecture to the UNet encoder and middle block (§2). As illustrated in Fig. 2 (blue bars), augmenting the base diffusion model with one ControlNet increases the serving latency by $1.55\times$, up from 2.9 seconds to 4.5 seconds. As more ControlNets are utilized by a request, their computational overhead accumulates. This is primarily due to the inefficient *sequential* ControlNet execution design in current T2I serving systems [42]: at each denoising step, the system sequentially computes the outputs of all the requested ControlNets before executing the base model (Fig. 7-Left).

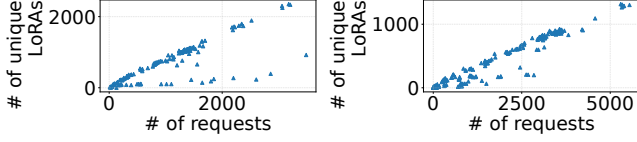


Figure 6: Scatter plots illustrating the number of requests received on each worker node (X-axis) against the number of unique LoRAs required by those requests (Y-axis). **Left:** Service A; **Right:** Service B.

3.2 LoRA Characterization

Prevalence. Similar to ControlNet, the vast majority of T2I requests utilize one or two LoRAs to stylize the generated image, as shown in Table 1. Specifically, over 90% of requests in Service A desire two LoRAs, while nearly 74% of requests in Service B demand one LoRA.

Long-tailed popularity. Compared to ControlNets, LoRAs have a significantly larger quantity but much smaller sizes. Our trace reports 6,908 distinct LoRAs for Service A and 7,463 LoRAs for Service B. Each LoRA is a few hundreds of MiB. Unlike ControlNets, the popularity of LoRAs follows a *long-tailed distribution* in both services; that is, a significant portion of invocations are contributed by a large number of *less popular* adapters, as illustrated in Fig. 4-Right,

Ineffective LoRA caching. Given the long-tailed popularity distribution of LoRAs, caching the top popular adapters in GPU memory offers *limited benefits*. To demonstrate this, we configure an LRU cache of varying size for LoRA caching. We replay the trace and measure the average number of times that the desired LoRAs are not available on GPU and must be brought from storage (i.e., cache miss) when serving two consecutive requests that demand different sets of LoRAs. As illustrated in Fig. 5 (orange curves), configuring a larger cache for LoRAs only results in a slight reduction of the loading overhead caused by cache miss. As another evidence, we analyze the production trace and depict in Fig. 6 a scatter plot illustrating the number of requests served on each node and the number of *unique* LoRAs required by these requests. We observe the linear correlation between the two numbers, invalidating the benefits of LoRA caching. As a result, production systems do not cache LoRAs but on-demand load them from local disk or a remote memory store, backed by a stable storage that manages LoRA weight files.

LoRA loading and patching overhead. Compared to ControlNets, LoRAs are compute-light and usually bottlenecked by the loading and patching overhead. Our measurements show that fetching two LoRAs with total size of approximately 800 MiB from a remote distributed cache takes more than one second. This overhead alone delays the base model serving by 34% (up from 2.9 seconds to 3.9 seconds). In addition, simply patching LoRA weights to the base model, as implemented in existing systems [27, 42], can be extremely inefficient, which we elaborate in §4.2.

3.3 Characterizing Base Model Serving

Currently, UNet-based diffusion models, such as SDXL [32], are predominately deployed to handle the majority of requests in production T2I services. These models are supported by a plethora of well-trained ControlNets [57] and LoRAs [19]. In the meantime, there is an emerging trend of deploying transformer-based diffusion models [12, 24] for improved image quality. As these models are recently developed, corresponding add-on modules remain lagging behind, with limited choices and availability. In this paper, we primarily focus on UNet-based models; our observations and optimization designs also apply to the transformer backbone (§4.4).

Limited benefits from batching. Diffusion model serving is computationally intensive, as evidenced by our experiments with varying batch sizes for an SDXL model [32] on NVIDIA A10, A100, and H800 GPUs (Fig. 8-Left). Across all three GPUs, doubling the batch size results in an approximately $2\times$ in serving latency, indicating minimal benefits from batching. In fact, generating a single image already saturates the computational resources of a high-end GPU. Consequently, production T2I services typically configure a constant batch size of 1 to minimize serving latency.

CFG dominates computation. To understand the computation of the base diffusion model, we break down its execution and find that over 90% of the execution time is spent on CFG computation (§2). Current CFG implementation employs *latent batching*. That is, in each denoising step, the latent tensor is duplicated and the two replicas are fed into the base model to perform conditional and unconditional denoising operations in *one batch*. However, as the two denoising operations are by nature compute-heavy, batching them together yields minimal benefits, leading to the similar performance with sequential execution even on a high-end GPU. In fact, latent batching results in up to $1.7\times$ slowdown in base model serving compared to an optimized design (§6.5).

3.4 Inefficiency of Current Serving Pipeline

To sum up, current T2I systems serve the base model and the requested add-on modules in a *sequential execution pipeline*. Specifically, assume a request utilizing m ControlNets and n LoRA adapters. Upon request arrival, the system loads all the desired ControlNets and LoRAs into GPU memory, followed by patching the n LoRAs to the base model. The system then encodes the text prompt and proceeds to the denoising process in N steps. At each step, it sequentially executes the m ControlNets and the LoRA-patched base model to generate a latent representation. The final latent representation is then sent to the VAE decoder to generate the output image. The end-to-end request serving latency is hence given by Eq. (1),

Notations	Description
$T_{Load}^{nL}, T_{Patch}^{nL}$	Time to load and patch n LoRA(s), respectively
T_{Load}^{mC}	Time to load m ControlNet(s)
T_{Enc}, T_{VAE}	Inference time of text encoder and the VAE decoder
T_{Comp}^{mC}	Inference time of m ControlNet(s)
T_{Comp}^B	Inference time of the base diffusion model
$T_{Comp}^{B'}$	Optimized inference time of the base diffusion model
ϵ_{Patch}^{nL}	Optimized latency for patching n LoRA(s)
δ_{Comp}^C	Overhead in ControlNet computation
δ_{Sync}^{mC}	Overhead in m ControlNet synchronization

Table 2: Notations to model T2I inference latency.

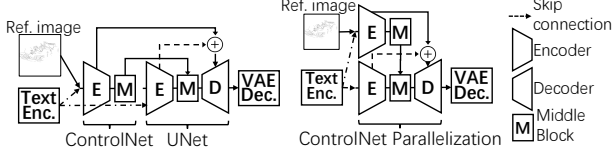


Figure 7: **Left:** Sequential ControlNet execution. **Right:** ControlNet parallelization.

where the notations are defined in Table 2:

$$T = \underbrace{T_{Load}^{mC} + T_{Load}^{nL} + T_{Patch}^{nL}}_{\text{time to load and patch add-on modules}} + \underbrace{T_{Enc} + \sum_{i=1}^N (T_{Comp}^{mC} + T_{Comp}^B) + T_{VAE}}_{\text{computation time}}. \quad (1)$$

Our characterization identifies efficiency issues concerning ControlNet loading (T_{Load}^{mC}), sequential ControlNet execution (T_{Comp}^{mC}), slow LoRA loading (T_{Load}^{nL}) and patching (T_{Patch}^{nL}), and inefficient latent batching in base model execution (T_{Comp}^B). We next address these issues with a holistic approach.

4 System Design

In this section, we propose SWIFTDIFFUSION, a system that efficiently serves the base diffusion model and the associated add-on modules through an optimized serving pipeline. To reduce the overhead of ControlNet loading and computation, SWIFTDIFFUSION introduces ControlNet-as-a-Service, which enables ControlNet caching and parallelization in a unified design (§4.1). To mitigate LoRA loading and patching overhead, SWIFTDIFFUSION overlaps LoRA fetching and base model execution at initial denoising steps, and uses an efficient method to quickly patch LoRA adapters (§4.2). SWIFTDIFFUSION also parallelizes CFG computation on multiple GPUs to expedite base model and ControlNet execution using a *latent parallelism* technique, together with kernel-level optimizations (§4.3). Collectively, these designs reduce the end-to-end T2I serving latency from Eq. (1) to

$$T = \epsilon_{Patch}^{nL} + T_{Enc} + \sum_{i=1}^N (T_{Comp}^{B'} + \delta_{Comp}^C + \delta_{Sync}^{mC}) + T_{VAE}. \quad (2)$$

In our evaluation, SWIFTDIFFUSION achieves up to $7.8\times$ reduction in latency and $1.6\times$ throughput improvement (§6.2). While we present SWIFTDIFFUSION primarily based on diffusion models with the UNet backbone, our design also applies to the recently proposed diffusion transformer (DiT) models [12, 24, 31], which we elaborate in §4.4.

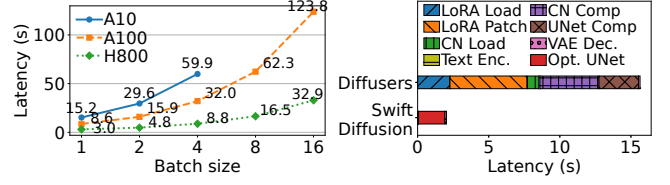


Figure 8: **Left:** SDXL inference saturates GPU. **Right:** Latency breakdown for a request with 3C/2L. CN: ControlNet.

4.1 ControlNet-as-a-Service

Motivation. Our characterization study (§3.1) reveals the widespread adoption of ControlNets. However, the existing system [42] falls short in supporting ControlNets by executing them and the base diffusion model sequentially (Fig. 7-Left). With more ControlNet(s) requested, the loading and computation delay accumulates linearly (Fig. 2).

ControlNet-as-a-Service. SWIFTDIFFUSION executes ControlNet(s) on dedicated GPUs and deploys them as a separate service by decoupling ControlNet execution from the base diffusion model. The data dependencies between ControlNet(s) and the base model allows them to execute in parallel on multiple GPUs (Fig. 7-Right). At each denoising step, the base model initiates the inference of UNet and concurrently invokes the requested ControlNet(s) by sending the reference image, latent tensor, and text embedding. Upon completion of serving the invocation, the ControlNet(s) becomes idle and available for the next invocation, thereby allowing a single ControlNet to be multiplexed by multiple base models. SWIFTDIFFUSION caches popular ControlNets in GPU memory to mitigate the loading overhead driven by the skewed distribution of ControlNet invocation (§3.1). ControlNet service can independently scale according to request traffic.

ControlNet parallelization. Without changing the data flow between ControlNets and the base model, SWIFTDIFFUSION partitions the entire computational graph into a *serial* part and a *parallel* part, as shown in Fig. 7. For the UNet-base SDXL model [32], the *serial* part consists of the one-time computation of the text encoder, one-time computation of the VAE decoder, and UNet decoder computation, while the *parallel* part consists of the computations of UNet’s encoder and ControlNet(s).

SWIFTDIFFUSION distributes the computational workload in the *parallel* part across multiple GPUs: the UNet is placed on one GPU while each ControlNet is allocated to a separate GPU and deployed as a service. At each denoising step, the UNet encoder and ControlNet(s) initiate computation concurrently. Upon completion of the UNet middle block inference, the UNet decoder *synchronously* awaits the outputs from ControlNet(s) before its computation, thereby strictly preserving the original data dependencies. Meanwhile, the ControlNet(s) becomes idle for next invocation. This parallel computing paradigm can achieve *close-to-ideal* speedup for two primary reasons. **First**, the computational load of a ControlNet closely

mirrors that of the UNet’s encoder blocks and middle block, given their shared model architectural design [57]. The only difference is that the ControlNet has additional zero convolution operators. Consequently, their computation times are nearly uniform when executed on the same type of GPU, leading to minimal idle time and high resource utilization. **Second**, communication between the ControlNet(s) and SDXL’s UNet is minimal, i.e., 108 MiB, when using high-performance communication links, e.g., NVLink [4]. The one-time data transmission incurs a *negligible* latency of less than 1 ms, ensuring efficient synchronization and minimal performance impact.

Deploy ControlNet service. Given the uniformity of computational load on each GPU, the speedup gains from ControlNet parallelization on multiple GPUs primarily subject to communication overhead. ControlNet parallelization necessitates high-performance inter-GPU bandwidth to achieve *close-to-ideal* speedup, as the outputs of ControlNets should be transmitted to the base model *synchronously* to complete base model inference.

With high inter-GPU bandwidth, e.g., NVLink [4] and InfiniBand [3], the communication overhead is negligible. Following Gustafson’s law [15], the ideal speedup of ControlNet parallelization with one ControlNet is $1.45\times$, while SWIFTDIFFUSION achieves $1.42\times$ with NVLink and $1.34\times$ with InfiniBand in a Nvidia H800 cluster. The optimality gap arises because ControlNet computation is $1.1\times$ longer than that of the UNet encoder and middle block. Similar results are observed in a Nvidia A100 cluster.

With low inter-GPU bandwidth, e.g., commodity Ethernet network, the communication overhead is remarkable. We run the SDXL model and a ControlNet, each on an AWS g5.2xlarge instances, which provides up to 10 Gbps network bandwidth. Under these conditions, ControlNet parallelization suffers from low bandwidth, only achieving $1.1\times$ speedup.

Summary. The performance of ControlNet service is bounded by inter-GPU bandwidth due to the *synchronous* communication between ControlNet(s) and base model.

ControlNet parallelization with low inter-GPU bandwidth. To mitigate the communication overhead, SWIFTDIFFUSION proposes a novel scheme to *pipeline ControlNet communication and base model computation*, or succinctly, *pipeline ControlNet*.

We observe that the outputs of ControlNet(s) between two adjacent denoising steps are highly similar, maintaining a similarity of over 0.99 almost all the time (Fig. 9-Left). Driven by the observation, SWIFTDIFFUSION establishes a *pipeline* scheme for ControlNet parallelization with low inter-GPU bandwidth, as shown in Fig. 10. At a denoising step t , the base model uses the ControlNet results at step $t - 1$, which have already been transmitted to the base model during the previous iteration, thereby avoiding the communication overhead. This approach results in a $1.25\times$ speedup compared to

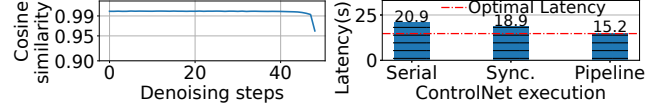


Figure 9: **Left:** Cosine similarities of ControlNet outputs between two adjacent steps. **Right:** Latency of generating an image using various ControlNet execution with low inter-GPU bandwidth.

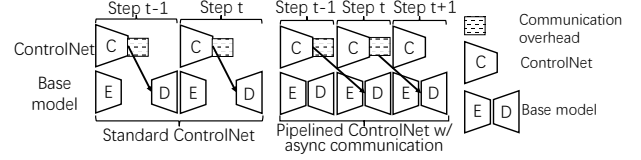


Figure 10: ControlNet parallelization with low inter-GPU bandwidth. We omit the middle blocks for simplicity.

the conventional *synchronous* scheme (Fig. 9-Right). Despite using one-step stale ControlNet results, our evaluation shows the generated images maintain comparable quality to those generated using standard workflow (§6.3).

Takeaways. Within ControlNet-as-a-Service, caching ControlNets eliminates the ControlNet loading overhead (T_{Load}^{mC} in Eqn. 1). ControlNet parallelization reduces the T_{Comp}^{mC} in Eqn. 1 to $\delta C_{\text{Comp}} + \delta_{\text{Sync}}^{mC}$ in Eqn. 2.

4.2 Efficient Text-to-Image with LoRAs

Motivation. As discussed in §3.2, LoRAs are stored in a local disk or remote cache system. To apply a LoRA for stylizing the image generation, the system typically takes two steps. First, it fetches the LoRA from storage and loads it into memory. After that, it patches the LoRA to the base diffusion model by merging its weights with the parameters of the base model. In existing system [42], the overhead of LoRA loading and patching is significant and accumulates with an increasing number of requested LoRAs (Fig. 2).

Bounded asynchronous LoRA loading (BAL). We analyze the progress of image generation and observe that the effect of LoRA is imperceptible during the initial denoising steps. We empirically validate this by executing the image generation process twice: once with LoRA patched on the diffusion model and once without. We collected and calculated the cosine similarity between the latent tensors (Fig. 3) generated with and without the LoRA at each denoising step, as demonstrated in Fig. 11-Left. The cosine similarities consistently exceed 0.99 during the initial denoising steps, indicating that LoRA exerts *minimal* effects during this stage. After step k , i.e., 20, in Fig. 11-Left, the similarity plunges, forming a bound that demarcates the latest possible time of LoRA patching. Fig. 12 further visualizes the denoising process of image generation with and without LoRA. The initial denoising steps constitute a semantics-planning stage [7, 25, 37, 60], wherein the model determines the image composition and

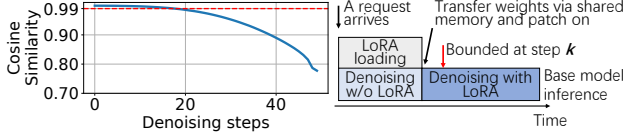


Figure 11: **Left:** Similarities between the latents generated with LoRA and those without LoRA. **Right:** Bounded asynchronous LoRA loading.

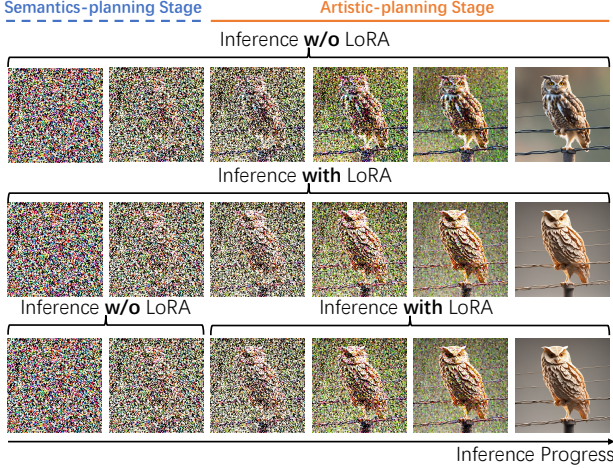


Figure 12: Images generated every 10 steps from the 0th step using a papercut LoRA [40]. **Prompt:** an owl standing on a wire. **Top:** W/o LoRA all the time. **Middle:** With LoRA all the time. **Bottom:** bounded async LoRA loading.

layout, generating visual semantics aligned with the text conditions [7, 60]. The remaining generation steps constitute an artistic-planning stage with image details gradually increasing, e.g., color, texture, and artistic style [7, 60]. Therefore, LoRA, as a method to change images’ styles and details, exerts minimal effects during the semantics-planning stage, corresponding with the high similarities between the latent tensors generated with and without the LoRA in Fig. 11-Left.

Driven by the observation, SWIFTDIFFUSION proposes overlapping the LoRA loading with the initial denoising stage, as shown in Fig. 11-Right. When a request arrives, SWIFTDIFFUSION initiates the asynchronous loading of the requested LoRA(s). Meanwhile, it *early-starts* the base stable diffusion model inference without LoRA patched. The asynchronous LoRA loading is bounded to guarantee that image quality will not be compromised. Specifically, at the k^{th} denoising step, if the requested LoRAs have not been loaded, the base model inference will halt and wait until the loading completes. Upon completion of the LoRA loading, SWIFTDIFFUSION patches the LoRA onto the base model by merging its weights with the parameters of the base model. The base model then proceeds with the remaining image generation process. SWIFTDIFFUSION executes LoRA loading in separate processes and utilizes shared memory to transfer LoRA weights from the loading processes to the base model serving process for efficient data transfer. When serving SDXL on an H800 GPU, a

LoRA with a size of 456 MiB is patched on the base model at the 11th denoising steps on average, with a minimal overhead (See 0C/0L and 0C/1L in Fig. 2). In cases where a request uses multiple LoRAs, SWIFTDIFFUSION launches multiple loading processes to load the LoRAs *in parallel*.

Analysis of k . The point at which a LoRA fully loaded and patched during the denoising process influences the extent of LoRA effects manifested in the generated image. Delaying LoRA patching leads to a diminished presence of LoRA effects in the generated images. SWIFTDIFFUSION employs a profiling method to determine the optimal value of k . Given a specific base model and LoRA, we calculate the cosine similarity between the latent tensors generated with and without the LoRA at each denoising step, akin to those in Fig. 11-Left. Then, we assign k to the step at which the similarity starts to drop below a predefined threshold, e.g., 0.99. On H800 and A100, LoRA loading mostly completes before step k , effectively hiding the loading overhead.

Efficient LoRA patching. Existing system [42] uses the PEFT [27] framework to merge LoRA weights with base model parameters. For a layer in the base stable diffusion model that will be patched with LoRA, PEFT *creates* a new LoRA layer to *replace* the original layer in the base model. The newly created LoRA layer augments the corresponding base model layer by incorporating LoRA weights and configurations. However, this *create_and_replace* operation incurs high overhead, taking 2 seconds for a LoRA of 341 MiB and occupying extra GPU memory. Though maintaining a separate copy of LoRA weights in the new augmented layer facilitates convenient LoRA training and efficiently patching off LoRA weights after image generation, SWIFTDIFFUSION finds it unnecessary. First, as a serving system, SWIFTDIFFUSION does not require the capability to support LoRA training. Besides, our characterization study reveals that the time interval between two consecutive requests is sufficient, i.e., longer than 1 second, to patch off LoRAs.

In SWIFTDIFFUSION, we merge LoRA weights with base model parameters in place, obtaining two benefits. It eliminates the latency overhead resulting from the *create_and_replace* operation and saves GPU memory for storing separate LoRA weights.

Takeaways. The designs of BAL and efficient LoRA patching reduces $T_{Load}^{nL} + T_{Patch}^{nL}$ in Eqn. 1 to ϵ_{Patch}^{nL} in Eqn. 2.

4.3 Optimized Base Model Execution

Motivation. We now shift our focus on the base diffusion model inference time, i.e., T_{Comp}^B in Eqn. 1, the last bottleneck in image generation. In fact, when the overhead of add-on modules is minimized, the base diffusion model inference accounts for over 93% of the end-to-end latency³. Moreover, the base diffusion model inference is computationally intensive,

³For SDXL inference on an H800 GPU.

and even a small batch size of 1 can saturate high-end GPUs (§3.3). To address this challenge, SWIFTDIFFUSION explores parallel computing to accelerate computation using multiple GPUs. Besides, SWIFTDIFFUSION incorporates kernel-level optimizations tailored for base diffusion model computation and its interaction with add-on modules, further enhancing performance.

Latent parallelism for diffusion model. The unique CFG technique used in image generation provides an opportunity for parallel computing. Recalling the diffusion model computation in §2, it involves denoising two latents to generate an image: one conditioned on texts and the other unconditionally. The two latents are then combined by computing a weighted sum, yielding an interpolated latent. The parallelism opportunity manifests in CFG, where the computation of denoising the two latents can be distributed across two separate GPUs, i.e., *latent parallelism*. Specifically, at each denoising step, SWIFTDIFFUSION duplicates the latent tensor (② in Fig. 3) and distributes the computations of the tensors across two GPUs, where each latent is fed into one base model on one GPU for conditioned or unconditioned denoising, respectively. With the same GPU type, the computations are uniform, and a *synchronous* communication interpolates the denoised latents through a weighted sum.

The simple yet effective latent parallelism strategy can accelerate the base diffusion model inference of a request by 1.4–1.9×, depending on the GPU capabilities and base model sizes. The performance gain is more pronounced with larger base models and lower-end GPUs, which we will elaborate in §6.5. Latent parallelism incurs little overhead, because 1) computations on different GPUs are uniform and finish at almost the same time, and 2) the communication overhead is minimal, mainly comprising the transfer of a small latent (< 1 MiB). Yet, the speedup achieved by latent parallelism may come at the expense of serving throughput when the denoising computation of a single latent does not saturate a GPU.

Compatibility with the add-on optimizations. Latent parallelism can be naturally applied during ControlNet computation, since ControlNets are architecturally similar to the base models (§4.1). Therefore, both of them can benefit from latent parallelism in the ControlNet-as-a-Service design. BAL can be seamlessly combined with latent parallelism. If the LoRA weights are not yet loaded, we allow the base models on both GPUs to early start denoising and simultaneously patch LoRAs when loading completes.

Kernel-level optimizations. SWIFTDIFFUSION includes several kernel-level optimizations to further enhance performance, including a customized CUDA Graph implementation and specialized CUDA kernels tailored to diffusion models. CUDA Graph is particularly suitable for T2I inference, as it uses a constant batch size of 1 (§3.3). Given the nearly homogeneous requested image resolutions in our production

environment, we only need to maintain a small number of CUDA Graphs resident in GPU memory. Further, we adapt the original CUDA graph to accommodate the ControlNet parallelization. Specifically, we tailor the base model and segment it as distinct CUDA Graphs according to its data dependencies with ControlNets. In addition to the existing optimized attention kernels [1], SWIFTDIFFUSION provides kernel optimizations specific to UNet-based diffusion models, including an optimized GELU activation operator by amalgamating GELU and matrix multiplication operations, and a fused operator that combines GroupNorm and SiLU operators to mask SiLU’s overhead.

Takeaways. Latent parallelism and kernel-level optimizations reduce T_{Comp}^B in Eqn. 1 to $T_{\text{Comp}}^{B'}$ in Eqn. 2.

4.4 Generalize to DiT-based Diffusion Models

First, the design of ControlNet parallelization can be effectively generalized to DiT-based diffusion models, such as SD3 [12] and Hunyuan-DiT [24], as the data dependencies between the ControlNet(s) and the base model in these architectures are analogous to those in UNet-based models. This architectural similarity enables the parallel execution of ControlNet(s) and base model inference in DiT-based models, employing the similar approach as in UNet-based models. Second, the advantages of efficient LoRA loading and patching can be effectively extended to accelerate image generation in DiT-based diffusion models, as these optimizations are agnostic to the underlying base model architecture. Third, DiT-based models also adopt CFG in denoising and benefit from latent parallelism. We validate our designs with DiT-based models in §6.7 and achieve consistent performance benefits.

5 Implementation

We have implemented SWIFTDIFFUSION on top of Diffusers [42], a PyTorch-based diffusion model inference framework that integrates state-of-the-art model optimization strategies. SWIFTDIFFUSION is written in 5.5k lines of Python and 2.4k lines of C++/CUDA code. ControlNet-as-a-Service, asynchronous LoRA loading, and latent parallelism are implemented in Python, while customized CUDA operators are developed in C++/CUDA. When a request arrives, separate processes are launched to LoRA weights asynchronously and transfer the weights to the base diffusion model serving process via shared memory.

6 Evaluation

We evaluate SWIFTDIFFUSION’s performance in terms of serving latency and image quality. Evaluation highlights include:

- SWIFTDIFFUSION achieves efficient serving performance without degrading image quality, outperforming strong state-of-the-art baselines, e.g., Nirvana [7] (§6.2).
- ControlNet-as-a-Service accelerates T2I serving with ControlNets, achieving a *close-to-ideal* speedup (§6.3).
- SWIFTDIFFUSION seamlessly incorporates LoRAs to stylize image generation while maintaining consistent serving latency (§6.4).
- SWIFTDIFFUSION has a $1.7\times$ speedup in base diffusion model inference with latent parallelism and kernel optimizations (§6.5).
- SWIFTDIFFUSION achieves up to $1.6\times$ throughput while using multiple GPUs compared with baselines (§6.6).
- SWIFTDIFFUSION generalizes to DiT-based diffusion models (§6.7).

6.1 Experimental Setup

Model and serving configurations. We adopt SDXL [32] as the primary base model for our experiments. The model and its variants have been widely used in our production cluster and benefit from comprehensive support for add-on modules. We use the default settings to generate images, with the number of denoising steps being 50 and resolution being 1024×1024 . The ControlNets [20] and LoRAs [39–41] used are publicly accessible in the HuggingFace repository. We serve SDXL and ControlNets with NVIDIA H800 GPUs.

Baselines. We re-implement Nirvana [7], the SOTA text-to-image serving system, and compare it with SWIFTDIFFUSION. The key idea behind Nirvana is to skip the first K denoising steps by utilizing a pre-cached image generated from a similar prompt to replace the randomly initialized noise latent (Fig. 3). By generating the image based on an intermediate representation instead of starting from scratch with noise, Nirvana aims to reduce the number of required denoising steps and improve serving latency. In our re-implementation, we prepare the pre-cached images using the same prompts that will be used to generate the images for quality evaluation.

Including Nirvana [7], we consider the following baselines:

- DIFFUSERS represents the standard text-to-image serving workflow incorporating ControlNets and LoRAs [42]. Images generated by DIFFUSERS adhere to the standard diffusion model inference process, which executes ControlNets sequentially and synchronously applies LoRA to the base diffusion model. While this approach yields images of standard quality, it incurs a relatively lengthy serving latency.
- NIRVANA-10 [7] omits ten denoising steps during image generation, i.e., $K = 10$.
- NIRVANA-20 [7] aggressively skips twenty denoising steps during image generation, i.e., $K = 20$.

Metrics. We evaluate each baseline in terms of *serving latency* and *image quality*. For serving latency, we measure the

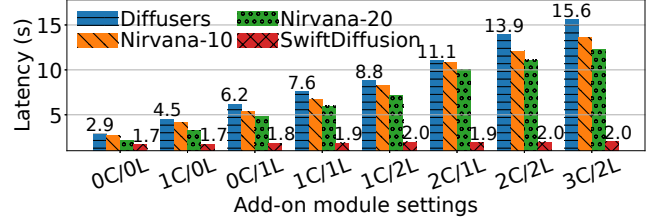


Figure 13: End-to-end serving latency with m ControlNets and n LoRAs (mC/nL).

end-to-end latency of generating an image based on a given text prompt. For image quality, we use the following quantitative metrics, which are considered essential and widely used in measuring image quality [7, 26, 32, 54, 59].

- CLIP [16, 33] score evaluates the alignment between generated images and their corresponding text prompts. A higher CLIP score indicates better alignment (\uparrow).
- Fréchet Inception Distance (FID) score [17] calculates the difference between two image sets, which correlates with human visual quality perception [7]. A low FID score means that two image sets are similar (\downarrow).
- Learned Perceptual Image Patch Similarity (LPIPS) score [59] quantifies the perceptual similarity between two images and has been demonstrated to closely align with human perception. A lower LPIPS score indicates that images are perceptually more similar (\downarrow).
- Structural Similarity Index Measure (SSIM) score [47] measures the similarity between two images, with a focus on the structural information in images. A higher SSIM score suggests a greater similarity between the images (\uparrow).

Like [7, 32], we conducted a user study with 75 participants to evaluate the image quality based on their visual perception.

Workloads. We use text prompts in Google’s PartiPrompts (P2) [54], which has a rich set of prompts in English. It has both simple and complex prompts across various categories (e.g., Animals, Scenes, and World Knowledge) and challenging aspects (e.g., Detail, Style, and Imagination). P2 has been widely used as a benchmark for image generation tasks [26, 32, 54]. For each request, we serve it with several add-on modules, following our production trace (Table 1).

6.2 End-to-End Performance

Serving latency. We measure requests’ average serving latency with different numbers of add-on modules and compare the results of each baseline in Fig. 13. SWIFTDIFFUSION shows its advantage across all settings that require add-on modules, achieving up to a $7.8\times$ speedup. SWIFTDIFFUSION outperforms other baselines by the ControlNet-as-a-Service design (§4.1) and efficient LoRA loading and patching (§4.2). In the absence of add-on modules, SWIFTDIFFUSION achieves a $1.7\times$ speedup compared to DIFFUSERS, due to *latent parallelism* and kernel optimizations (§4.3).



Figure 14: Real examples of generated images by DIFFUSERS [42], SWIFTDIFFUSION, and NIRVANA-10 [7].

Image Quality. We compare the quality of images generated by each baseline. Since our ControlNets-as-a-Service design does not make any differences in the generated image content, we focus on evaluating the LoRA effects. Two settings are considered: the first uses a single LoRA to generate images in a papercut style [40], while the second employs two LoRAs to generate images in a combination of William Eggleston photography style and filmic style [39, 41]. We use the prompts in P2 [54] that emphasize vivid details in images.

1) Quantitative evaluation. Table 3 shows the CLIP scores achieved by each baseline, which measure the alignment between generated images and their corresponding prompts. The results indicate that all baselines exhibit comparable performance in terms of alignment.

Table 4 shows the FID, LPIPS, and SSIM scores achieved by each baseline. These metrics focus on comparing the generated images with the real images (“ground truth”). Therefore, we use the images generated by DIFFUSERS as the ground truth, as it represents the original T2I serving workflow, while NIRVANA-10, NIRVANA-20, and SWIFTDIFFUSION introduce slight modifications to accelerate the image generation. We also consider a new baseline NOLORA, which does not employ any LoRAs in image generation. We can see that SWIFTDIFFUSION outperforms other baselines, achieving the best performance across all metrics. NIRVANA-10 and NIRVANA-20 fall short because they generate an image based on the contents of a cached image, which is selected only based on the prompt similarity. Even with the same prompt, the visual contents in cached images can be drastically different (See Fig. 1-Left) and may not align with the style of LoRAs. Fig. 14 presents real examples generated by DIFFUSERS, NIRVANA-10, and SWIFTDIFFUSION, illustrating that images generated by DIFFUSERS and SWIFTDIFFUSION are visually almost indistinguishable, while NIRVANA-10 fails to match the quality of DIFFUSERS.

2) Qualitative evaluation. We conducted a user study involving 75 participants to compare the quality of images gen-

Setting	DIFFUSERS	NIRVANA-10	NIRVANA-20	SWIFTDIFFUSION
1	34.3	33.7	34.2	33.9
2	33.9	32.7	32.3	33.7

Table 3: CLIP (\uparrow) scores.

LoRA Setting	Baseline	FID (\downarrow)	LPIPS (\downarrow)	SSIM (\uparrow)
One LoRA: Papercut [40]	NOLORA	2.71	0.44	0.59
	NIRVANA-10	2.66	0.57	0.42
	NIRVANA-20	3.47	0.61	0.41
	SWIFTDIFFUSION	0.53	0.26	0.74
Two LoRAs: Filmic [39] + Photography [41]	NOLORA	1.27	0.45	0.63
	NIRVANA-10	2.19	0.57	0.48
	NIRVANA-20	2.25	0.62	0.44
	SWIFTDIFFUSION	0.78	0.29	0.75

Table 4: Quantitative evaluation on image quality.

erated based on human visual perception. We consider DIFFUSERS, NIRVANA-10, and SWIFTDIFFUSION in this part. Inspired by Chatbot Arena [61], we constructed an online arena that *randomly* presents two images to users, offering four options: both images are acceptable, neither image is acceptable, image 1 is acceptable, or image 2 is acceptable. Participants made their selections based on both the degree of image alignment with the prompt and their subjective aesthetic preferences. We collected over 1.2k data points. The findings indicate that our method is capable of producing images of the same quality as DIFFUSERS, both with a 70% acceptance rate. In contrast, NIRVANA-10 has an overall acceptance rate below 50% due to its skipped denoising steps and not considering the impact of add-on modules during the match process.

6.3 ControlNet-as-a-Service

This section evaluates the performance of ControlNets-as-a-service design at a micro-benchmark level, isolating it from our LoRA design and optimizations in base model. We compare DIFFUSERS and SWIFTDIFFUSION, as Nirvana [7] lacks specialized designs for ControlNets. Fig. 15-Left illustrates the serving latency achieved by DIFFUSERS and SWIFTDIFFUSION, where SWIFTDIFFUSION achieves up to $2.2\times$ speedup by distributing ControlNets computation across multiple GPUs. Notably, SWIFTDIFFUSION’s design does not alter the image generation process, ensuring that the images generated by DIFFUSERS and SWIFTDIFFUSION are identical.

To further analyze SWIFTDIFFUSION’s speedup, we employ Gustafson’s law [15], which quantifies the theoretical speedup in execution time for a task that benefits from parallel computing. Let N denote the number of processors, and let s and p represent the fractions of time spent executing the serial and parallel parts of the program, i.e., $s + p = 1$. The theoretical speedup S from parallel computing is $S = s + p \times N$ [49]. In the context of T2I generation with ControlNets, the serial parts comprise the computation of decoder blocks in UNet, while the parallel parts include the computation of UNet’s encoder blocks together with middle block, and ControlNets

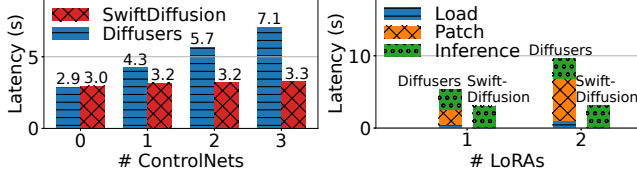


Figure 15: **Left:** Microbenchmark on ControlNets. **Right:** Microbenchmark on LoRAs.

	CLIP (\uparrow)	FID (\downarrow)	LPIPS (\downarrow)	SSIM (\uparrow)
Sync	34.1	0.66	0.28	0.75
Pipeline	34.6	0.45	0.33	0.71

Table 5: Quantitative evaluation on image quality.

(§4.1). When using three ControlNets, the serial parts account for $s = 0.55$ and the parallel parts take $p = 0.45$, indicating a theoretical speedup of $2.35\times$. SWIFTDIFFUSION’s achieved $2.2\times$ speedup closely approaches this theoretical limit, demonstrating its effectiveness in leveraging parallelism across multiple GPUs.

ControlNet-as-a-Service with low inter-GPU bandwidth. We next evaluate the latency performance and image quality of ControlNet-as-a-Service deployed over a commodity Ethernet network. We run SWIFTDIFFUSION on AWS g5.2xlarge instances, which provide up to 10 Gbps network bandwidth [9]. Fig. 9-Right presents the serving latency with one ControlNet, where the pipeline ControlNet achieves *close-to-ideal* latency performance. Table 5 shows the image quality metrics, which are derived as those in §6.2. Images generated using pipeline ControlNet are comparable to those using sync ControlNet.

6.4 Efficient T2I with LoRAs

This section evaluates SWIFTDIFFUSION’s design for efficient image generation with LoRAs at a micro-benchmark level, excluding other optimizations. We also exclude Nirvana [7] since it does not have specialized designs for LoRAs. As described in §4.2, DIFFUSERS requires two steps to patch on a LoRA: first, loading the LoRA from a local disk or remote in-memory caching system, and then creating a new LoRA layer and replacing the corresponding layer in the base model to merge the LoRA weights [27]. This process incurs a high latency overhead, as shown in Fig. 15, with up to a $2.3\times$ increase in serving latency when using two LoRAs. For the single LoRA case, we use a LoRA of 341 MiB. For the two LoRA cases, we use LoRAs of 341 MiB and 456 MiB. Fig. 15-Right shows that SWIFTDIFFUSION’s design significantly reduces the overhead of LoRA loading and patching to 230 ms through its efficient design (§4.2), nearly eliminating the overhead. The image quality evaluation in §6.2 shows that SWIFTDIFFUSION can generate high-quality images that rival those of DIFFUSERS.

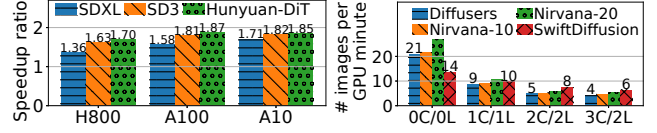


Figure 16: **Left:** Speedup ratio of latent parallelism on different GPU types and base models. **Right:** Serving throughput with m ControlNets and n LoRAs (mC/nL).

6.5 Optimize Base Model Inference

This section evaluates SWIFTDIFFUSION’s optimizations on the base diffusion model inference without adding any add-on modules, thereby disabling all optimizations for ControlNets and LoRAs. As Nirvana’s design only affects the number of denoising steps, we primarily compare SWIFTDIFFUSION with DIFFUSERS. In §4.3, we introduce two main techniques to optimize base model inference: latent parallelism and kernel-level optimization. Fig. 16-Left shows the speedup ratio achieved by latent parallelism, where kernel-level optimizations are disabled. The gains of latent parallelism are more pronounced on GPUs with lower compute capabilities, achieving speedup ratios of $1.36\times$, $1.58\times$, and $1.71\times$ on H800, A100, and A10, respectively. On the basis of latent parallelism, the kernel-level optimizations, including CUDA graph and optimized kernel operators, collectively contribute to $1.24\times$ speedup.

6.6 Serving Throughput on GPUs

SWIFTDIFFUSION is primarily designed to minimize serving latency, but it also achieves superior serving throughput when augmented with add-on modules. Fig. 16-Right illustrates the request serving throughput of each baseline, measured as the number of images generated per minute of GPU time. SWIFTDIFFUSION achieves up to a $1.6\times$ higher throughput compared to other baselines with 2C/2L, benefiting from its efficient design of LoRA loading and patching (§4.2). This demonstrates SWIFTDIFFUSION’s ability to greatly reduce serving latency (Fig. 13) while maintaining high throughput. With 0C/0L, SWIFTDIFFUSION has lower throughput as a single latent computation does not saturate GPU. NIRVANA-20 sometimes achieves good throughput due to its aggressive design, albeit at the cost of compromising image quality.

6.7 Generalization to DiT-based SD Model

We evaluate our designs on DiT-based diffusion models. We use SD3 [12], Hunyuan-DiT [24], and their add-on modules.

ControlNet-as-a-Service speeds up DiT-based T2I inference with ControlNet, close to the theoretical speedup gains according to the Gustafson’s law [15]. With SD3 [12], SWIFTDIFFUSION achieves a $1.46\times$ speedup, rivaling the theoretically $1.50\times$ speedup. With Hunyuan-DiT [24], SWIFTDIF-

	CLIP (\uparrow)	FID (\downarrow)	LPIPS (\downarrow)	SSIM (\uparrow)
SD3	33.9/33.0	0.07/7.50	0.60/0.65	0.41/0.40
Hunyuan-DiT	34.9/34.0	0.12/2.36	0.40/0.49	0.57/0.49

Table 6: Image quality evaluation with SWIFTDIFFUSION/NoLoRA

FUSION achieves a $1.23\times$ speedup, rivaling the theoretically $1.27\times$ speedup.

Bounded async LoRA loading. We evaluate the generated image quality quantitatively while enabling BAL on DiT-based models. We compare SWIFTDIFFUSION and NoLoRA and derive the metrics as those in §6.2 in Table 6. SWIFTDIFFUSION consistently outperforms and generates high-quality images.

Latent parallelism. Fig. 16-Left shows the achieved speedup from latent parallelism on DiT-based models, which is consistent to that of UNet-based models.

7 Related Works

Model serving systems. Existing research on model serving systems focuses on reducing latency [11, 28, 45, 50, 51], improving throughput [8, 50], enhancing performance predictability [13, 56], and conserving resources [14, 43, 55]. These studies concentrate on optimizing various workloads, including graph neural networks [46], recommendation models [51], and large language models [28, 45, 53]. Our work is orthogonal to the aforementioned efforts, as T2I models have drastically different computation intensity and workflow.

T2I diffusion model inference. Diffusers [42] is an out-of-the-box inference framework that incorporates state-of-the-art optimization strategies tailored for diffusion models. Deep-Cache [26] leverages the temporal consistency of high-level features to reduce redundant computations. DistriFusion [22] facilitates the parallel execution of diffusion models across multiple GPUs. Nirvana [7] employs approximate caching to skip a certain number of denoising steps. Yet, these works only optimize the base model inference and overlook the significant latency overhead introduced by add-on modules, which can be $4\times$ higher than that of the base model inference. Our work conducts a pioneering analysis of the status quo in production diffusion model deployment. Driven by real-world traces, we address the system inefficiencies caused by incorporating add-on modules. Notably, the existing optimizations for the base model can be seamlessly integrated.

Serving systems with add-on modules. In the domain of large language models, cutting-edge research [10, 23, 36] has proposed efficient inference techniques for models with add-on modules (i.e., LoRAs), such as CUDA-optimized operators for batched LoRA computations on GPUs and efficient GPU memory management mechanisms. These works aim to enable multi-tenant sharing of the base model to accommodate more LoRA adapters within the same batch. Yet, batching

yields *minimal* benefits in diffusion model inference, due to its compute-intensive nature. Thus, these multi-tenant optimization strategies work ineffectively in our scenario. In addition to LoRA, these works also overlook ControlNet, a specialized add-on module in diffusion model inference.

8 Conclusion

We present SWIFTDIFFUSION, an efficient T2I serving workflow that augments image generation with ControlNets and LoRAs. Guided by a production characterization of commercial T2I services, SWIFTDIFFUSION introduces three novel designs. Firstly, it deploys ControlNets as a service to accelerate loading and inference. Secondly, SWIFTDIFFUSION overlaps LoRA loading with base model inference and efficiently patches weights. Last, it optimizes the base model inference. Compared to existing systems, SWIFTDIFFUSION achieves up to a $7.8\times$ latency reduction and a $1.6\times$ increased throughput while maintaining image quality.

References

- [1] Accelerate inference of text-to-image diffusion models. https://huggingface.co/docs/diffusers/en/tutorials/fast_diffusion#accelerate-inference-of-text-to-image-diffusion-models, 2024.
- [2] Fooocus inpaint. <https://github.com/lillyasviel/Fooocus>, 2024.
- [3] NVIDIA InfiniBand Switch Systems User Manual. <https://bit.ly/3XJL25n>, 2024.
- [4] NVIDIA NVLink: High-speed GPU interconnect. <https://www.nvidia.com/en-us/design-visualization/nvlink-bridges/>, 2024.
- [5] Adobe. Adobe unleashes new era of creativity for all with the commercial release of generative AI. <http://bit.ly/3Xwfa2C>, 2023.
- [6] Adobe. Dream bigger with adobe firefly. <https://www.adobe.com/sensei/generative-ai/firefly.html/>, 2024.
- [7] Shubham Agarwal, Subrata Mitra, Sarthak Chakraborty, Srikrishna Karanam, Koyel Mukherjee, and Shiv Kumar Saini. Approximate caching for efficiently serving text-to-image diffusion models. In *Proc. USENIX NSDI*, 2024.
- [8] Sohaib Ahmad, Hui Guan, Brian D. Friedman, Thomas Williams, Ramesh K. Sitaraman, and Thomas Woo. Proteus: A high-throughput inference-serving system with accuracy scaling. In *Proc. ACM ASPLOS*, 2024.

- [9] Amazon. Amazon ec2 g5 instances. <https://aws.amazon.com/ec2/instance-types/g5/>, 2024.
- [10] Lequn Chen, Zihao Ye, Yongji Wu, Danyang Zhuo, Luis Ceze, and Arvind Krishnamurthy. Punica: Multi-tenant LoRA serving. In *Proc. MLSys*, 2024.
- [11] Daniel Crankshaw, Xin Wang, Guilio Zhou, Michael J. Franklin, Joseph E. Gonzalez, and Ion Stoica. Clipper: A low-latency online prediction serving system. In *Proc. USENIX NSDI*, 2017.
- [12] Patrick Esser, Sumith Kulal, Andreas Blattmann, Rahim Entezari, Jonas Müller, Harry Saini, Yam Levi, Dominik Lorenz, Axel Sauer, Frederic Boesel, Dustin Podell, Tim Dockhorn, Zion English, and Robin Rombach. Scaling rectified flow transformers for high-resolution image synthesis. In *Proc. ICML*, 2024.
- [13] Arpan Gujarati, Reza Karimi, Safya Alzayat, Wei Hao, Antoine Kaufmann, Ymir Vigfusson, and Jonathan Mace. Serving DNNs like Clockwork: Performance predictability from the bottom up. In *Proc. USENIX OSDI*, 2020.
- [14] Jashwant Raj Gunasekaran, Cyan Subhra Mishra, Prashanth Thinakaran, Bikash Sharma, Mahmut Taylan Kandemir, and Chita R. Das. Cocktail: A multidimensional optimization for model serving in cloud. In *Proc. USENIX NSDI*, 2022.
- [15] John L. Gustafson. Reevaluating amdahl’s law. *Commun. ACM*, 1988.
- [16] Jack Hessel, Ari Holtzman, Maxwell Forbes, Ronan Le Bras, and Yejin Choi. CLIPScore: A reference-free evaluation metric for image captioning. In Marie-Francine Moens, Xuanjing Huang, Lucia Specia, and Scott Wen-tau Yih, editors, *Proc. EMNLP*, 2021.
- [17] Martin Heusel, Hubert Ramsauer, Thomas Unterthiner, Bernhard Nessler, and Sepp Hochreiter. Gans trained by a two time-scale update rule converge to a local nash equilibrium. In *Proc. NIPS*, 2017.
- [18] Jonathan Ho and Tim Salimans. Classifier-free diffusion guidance. In *NeurIPS 2021 Workshop on Deep Generative Models and Downstream Applications*, 2021.
- [19] Edward J Hu, yelong shen, Phillip Wallis, Zeyuan Allen-Zhu, Yuanzhi Li, Shean Wang, Lu Wang, and Weizhu Chen. LoRA: Low-rank adaptation of large language models. In *Proc. ICLR*, 2022.
- [20] HuggingFace. Huggingface diffusers sdxl controlnets. <https://huggingface.co/diffusers/controlnet-depth-sdxl-1.0>, 2024.
- [21] Xuan Ju, Xian Liu, Xintao Wang, Yuxuan Bian, Ying Shan, and Qiang Xu. BrushNet: a plug-and-play image inpainting model with decomposed dual-branch diffusion. In *Proc. ECCV*, 2024.
- [22] Muyang Li, Tianle Cai, Jiaxin Cao, Qinsheng Zhang, Han Cai, Junjie Bai, Yangqing Jia, Ming-Yu Liu, Kai Li, and Song Han. DistriFusion: Distributed parallel inference for high-resolution diffusion models. In *Proc. IEEE/CVF CVPR*, 2024.
- [23] Suyi Li, Hanfeng Lu, Tianyuan Wu, Minchen Yu, Qizhen Weng, Xusheng Chen, Yizhou Shan, Binhang Yuan, and Wei Wang. CaraServe: CPU-assisted and rank-aware LoRA serving for generative LLM inference. *arXiv preprint arXiv:2401.11240*, 2024.
- [24] Zhimin Li, Jianwei Zhang, Qin Lin, Jiangfeng Xiong, Yanxin Long, Xincheng Deng, Yingfang Zhang, Xingchao Liu, Minbin Huang, Zedong Xiao, et al. Hunyuan-DiT: A powerful multi-resolution diffusion transformer with fine-grained chinese understanding. *arXiv preprint arXiv:2405.08748*, 2024.
- [25] Haozhe Liu, Wentian Zhang, Jinheng Xie, Francesco Faccio, Mengmeng Xu, Tao Xiang, Mike Zheng Shou, Juan-Manuel Perez-Rua, and Jürgen Schmidhuber. Faster diffusion via temporal attention decomposition. *arXiv preprint arXiv:2404.02747*, 2024.
- [26] Xinyin Ma, Gongfan Fang, and Xinchao Wang. Deep-Cache: Accelerating diffusion models for free. In *Proc. IEEE/CVF CVPR*, 2024.
- [27] Sourab Mangrulkar, Sylvain Gugger, Lysandre Debut, Younes Belkada, Sayak Paul, and Benjamin Bossan. PEFT: State-of-the-art parameter-efficient fine-tuning methods. <https://github.com/huggingface/peft>, 2022.
- [28] Xupeng Miao, Gabriele Oliaro, Zhihao Zhang, Xinhao Cheng, Zeyu Wang, Zhengxin Zhang, Rae Ying Yee Wong, Alan Zhu, Lijie Yang, Xiaoxiang Shi, Chunan Shi, Zhuoming Chen, Daiyaan Arfeen, Reyna Abhyankar, and Zhihao Jia. SpecInfer: Accelerating large language model serving with tree-based speculative inference and verification. In *Proc. ACM ASPLOS*, 2024.
- [29] Midjourney. Midjourney ai. <https://www.midjourney.com/explore>, 2024.
- [30] OpenAI. DALL·E 2. <https://openai.com/index/dall-e-2/>, 2024.
- [31] William Peebles and Saining Xie. Scalable diffusion models with transformers. In *Proc. ICCV*, 2023.
- [32] Dustin Podell, Zion English, Kyle Lacey, Andreas Blattmann, Tim Dockhorn, Jonas Müller, Joe Penna, and

- Robin Rombach. SDXL: Improving latent diffusion models for high-resolution image synthesis. In *Proc. ICLR*, 2024.
- [33] Alec Radford, Jong Wook Kim, Chris Hallacy, Aditya Ramesh, Gabriel Goh, Sandhini Agarwal, Girish Sastry, Amanda Askell, Pamela Mishkin, Jack Clark, Gretchen Krueger, and Ilya Sutskever. Learning transferable visual models from natural language supervision. In *Proc. ICML*, 2021.
- [34] Robin Rombach, Andreas Blattmann, Dominik Lorenz, Patrick Esser, and Björn Ommer. High-resolution image synthesis with latent diffusion models. In *Proc. IEEE/CVF CVPR*, 2022.
- [35] Olaf Ronneberger, Philipp Fischer, and Thomas Brox. U-Net: Convolutional networks for biomedical image segmentation. In *Proc. MICCAI*, 2015.
- [36] Ying Sheng, Shiyi Cao, Dacheng Li, Coleman Hooper, Nicholas Lee, Shuo Yang, Christopher Chou, Banghua Zhu, Lianmin Zheng, Kurt Keutzer, Joseph E. Gonzalez, and Ion Stoica. S-LoRA: Serving thousands of concurrent LoRA adapters. In *Proc. MLSys*, 2023.
- [37] Chenyang Si, Ziqi Huang, Yuming Jiang, and Ziwei Liu. Freeu: Free lunch in diffusion u-net. In *CVPR*, 2024.
- [38] Kolers Team. Kolers: Effective training of diffusion model for photorealistic text-to-image synthesis. https://github.com/Kwai-Kolors/Kolors/commits/master/imgs/Kolors_paper.pdf, 2024.
- [39] TheLastBen. Filmic. <https://huggingface.co/TheLastBen/Filmic>, 2024.
- [40] TheLastBen. Papercut sdxl. https://huggingface.co/TheLastBen/Papercut_SDXL, 2024.
- [41] TheLastBen. William eggleson style sdxl. https://huggingface.co/TheLastBen/William_Eggleson_Style_SDXL, 2024.
- [42] Patrick von Platen, Suraj Patil, Anton Lozhkov, Pedro Cuenca, Nathan Lambert, Kashif Rasul, Mishig Davaadorj, Dhruv Nair, Sayak Paul, William Berman, Yiyi Xu, Steven Liu, and Thomas Wolf. Diffusers: State-of-the-art diffusion models. <https://github.com/huggingface/diffusers>, 2022.
- [43] Luping Wang, Lingyun Yang, Yinghao Yu, Wei Wang, Bo Li, Xianchao Sun, Jian He, and Liping Zhang. Morphling: Fast, near-optimal auto-configuration for cloud-native model serving. In *Proc. ACM SoCC*, 2021.
- [44] Qixun Wang, Xu Bai, Haofan Wang, Zekui Qin, Anthony Chen, Huaxia Li, Xu Tang, and Yao Hu. InstantID: Zero-shot identity-preserving generation in seconds. *arXiv preprint arXiv:2401.07519*, 2024.
- [45] Yiding Wang, Kai Chen, Haisheng Tan, and Kun Guo. Tabi: An efficient multi-level inference system for large language models. In *Proc. ACM EuroSys*, 2023.
- [46] Yuke Wang, Boyuan Feng, Zheng Wang, Tong Geng, Kevin Barker, Ang Li, and Yufei Ding. MGG: Accelerating graph neural networks with fine-grained intra-kernel communication-computation pipelining on multi-GPU platforms. In *Proc. USENIX OSDI*, 2023.
- [47] Zhou Wang, Alan C Bovik, Hamid R Sheikh, and Eero P Simoncelli. Image quality assessment: From error visibility to structural similarity. *IEEE Transactions on Image Processing*, 2004.
- [48] Zijie J. Wang, Evan Montoya, David Munechika, Haoyang Yang, Benjamin Hoover, and Duen Horng Chau. DiffusionDB: A large-scale prompt gallery dataset for text-to-image generative models. In *Proc. ACL*, 2023.
- [49] Wikipedia. Gustafson’s law. https://en.wikipedia.org/wiki/Gustafson%27s_law, 2024.
- [50] Yanan Yang, Laiping Zhao, Yiming Li, Huanyu Zhang, Jie Li, Mingyang Zhao, Xingzhen Chen, and Keqiu Li. INFless: A native serverless system for low-latency, high-throughput inference. In *Proc. ACM ASPLOS*, 2022.
- [51] Haojie Ye, Sanketh Vedula, Yuhang Chen, Yichen Yang, Alex Bronstein, Ronald Dreslinski, Trevor Mudge, and Nishil Talati. GRACE: A scalable graph-based approach to accelerating recommendation model inference. In *Proc. ACM ASPLOS*, 2023.
- [52] Hu Ye, Jun Zhang, Sibao Liu, Xiao Han, and Wei Yang. IP-Adapter: Text compatible image prompt adapter for text-to-image diffusion models. *arXiv preprint arXiv:2308.06721*, 2023.
- [53] Gyeong-In Yu, Joo Seong Jeong, Geon-Woo Kim, Soojeong Kim, and Byung-Gon Chun. Orca: A distributed serving system for transformer-based generative models. In *Proc. USENIX OSDI*, 2022.
- [54] Jiahui Yu, Yuanzhong Xu, Jing Yu Koh, Thang Luong, Gunjan Baid, Zirui Wang, Vijay Vasudevan, Alexander Ku, Yinfei Yang, Burcu Karagol Ayan, Ben Hutchinson, Wei Han, Zarana Parekh, Xin Li, Han Zhang, Jason Baldridge, and Yonghui Wu. Scaling autoregressive models for content-rich text-to-image generation. *Transactions on Machine Learning Research*, 2022.
- [55] Chengliang Zhang, Minchen Yu, Wei Wang, and Feng Yan. MArk: Exploiting cloud services for cost-effective, SLO-aware machine learning inference serving. In *Proc. USENIX ATC*, 2019.

- [56] Hong Zhang, Yupeng Tang, Anurag Khandelwal, and Ion Stoica. SHEPHERD: Serving DNNs in the wild. In *Proc. USENIX NSDI*, 2023.
- [57] Lvmin Zhang, Anyi Rao, and Maneesh Agrawala. Adding conditional control to text-to-image diffusion models. In *Proc. IEEE/CVF ICCV*, 2023.
- [58] Lvmin Zhang, Anyi Rao, and Maneesh Agrawala. IC-Light. <https://github.com/Illyasviel/IC-Light>, 2024.
- [59] Richard Zhang, Phillip Isola, Alexei A Efros, Eli Shechtman, and Oliver Wang. The unreasonable effectiveness of deep features as a perceptual metric. In *Proc. IEEE/CVF CVPR*, 2018.
- [60] Yuxin Zhang, Weiming Dong, Fan Tang, Nisha Huang, Haibin Huang, Chongyang Ma, Tong-Yee Lee, Oliver Deussen, and Changsheng Xu. Prospect: Prompt spectrum for attribute-aware personalization of diffusion models. *ACM Trans. Graph.*, 2023.
- [61] Lianmin Zheng, Wei-Lin Chiang, Ying Sheng, Siyuan Zhuang, Zhanghao Wu, Yonghao Zhuang, Zi Lin, Zhuohan Li, Dacheng Li, Eric. P Xing, Hao Zhang, Joseph E. Gonzalez, and Ion Stoica. Judging LLM-as-a-judge with MT-Bench and Chatbot Arena. In *Proc. NeurIPS Datasets and Benchmarks Track*, 2023.